Medicinal Chemistry Research (2022) 31:2119–2131
https://doi.org/10.1007/s00044-022-02974-z

MEDICINAL CHEMISTRY RESEARCH

ORIGINAL RESEARCH

Synthesis, biological evaluation, and bioinformatics analysis of indole analogs on AChE and GST activities

Adnan Cetin[1] · Mesut Toptas[2] · Fikret Türkan[3]

Received: 27 July 2022 / Accepted: 11 September 2022 / Published online: 21 September 2022
© The Author(s), under exclusive licence to Springer Science+Business Media, LLC, part of Springer Nature 2022

Abstract

In this article, we aimed to (1) synthesize novel 3-substitue 2-methyl indole analogs, and (2) evaluate their biological activities against Acetylcholinesterase enzyme (AChE) and Glutathione S-transferase enzyme (GST), (3) predict ADMET and pharmacokinetic properties of the 3-substitue 2-methyl indole analogs (4) reveal the possible interactions between 3-substitue 2-methyl indole analogs and selected enzymes. In vitro enzyme inhibition studies revealed the 3-substitue 2-methyl indole analogs exhibited moderate to good inhibitory activities against AChE and GST enzymes. 2-azido-1-(2-methyl-1H-indol-3-yl) ethanone synthesized was a good inhibitor with the lowest Ki value for both enzymes. Furthermore, a molecular docking study of 3-substitue 2-methyl indole analogs was carried out in the active site of AChE/GST to gain insight into the interaction modes of the synthesized analogs and rationalized structure-activity relationship. The binding energies of the AChE-3-substitue 2-methyl indole analogs' complexes were found between −9.3 and −6.0 kcal/mol, and the binding energies of the GST-3-substitue 2-methyl indole analogs' complexes were also found between −11.1 and −7.5 kcal/mol.

Graphical abstract

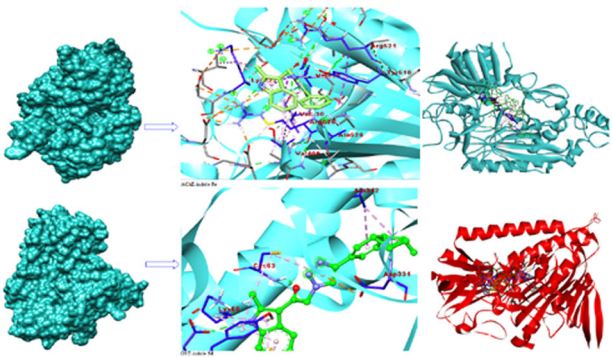

Keywords Alzheimer · Docking · Enzyme inhibition · Pharmacokinetic · Spectroscopy · Synthesis

Supplementary information The online version contains supplementary material available at https://doi.org/10.1007/s00044-022-02974-z.

✉ Adnan Cetin
adnancetin@yyu.edu.tr

[1] Department of Chemistry, Faculty of Education, University of Van Yuzuncu Yil, Van 65250, Turkey

[2] Department of Chemistry, Faculty of Art and Science, University of Mus Alparslan, Mus 49250, Turkey

[3] Department of Basic Sciences, Faculty of Dentistry, Iğdır University, Iğdır 76000, Turkey

Highlights

- New derivatives of the substituted 3-substitue 2-methyl indole analogs were synthesized.
- Discovery of the indole analogs as potential inhibitor of the AChE and GST receptors.
- The substituted indole analogs: molecular docking studies and pharmacokinetics.
- Lead drug discovery using molecular docking for the selected enzymes.

Introduction

AChE was extensively pursued as drug-targets with respect to a diverse array of brain diseases related medical conditions, such as Alzheimer's (AD), Parkinson's diseases, depression, and Amyotrofik Lateral Skleroz [1]. This is most likely due to its high prevalence in the human brain and that enzyme plays an important role in many biological functions particularly, central nervous system functions. Furthermore, ACh enzymes were indicated as targets for a vast range of therapeutic applications including pharmacotherapy for autism, tobacco dependency and depression [2, 3]. GSTs enzymes that belong to the receptor super important family in the cellular antioxidant system, have these receptors, and they were used to reduce glutathione for scavenge potentially toxic substances that have catalyzed the conjugation of reduced glutathione to electrophilic xenobiotics for maintaining cellular homeostasis [4–7]. The development of new drugs with potential therapeutic applications was one of the complex and difficult processes in the pharmaceutical industry. A tremendous economic cost has been devoted to the discovery of new therapeutic agents. The activity of a drug is the result of many factors such as bioavailability, toxicity and metabolism. The rational drug design has been an important scientific subject [8]. All the scientific studies related to drug discovery were valuable as both the potential benefits to human health and reduces the enormous costs in terms of time and economy [9]. The presence of various substituents at certain positions of the molecules was very important in terms of drug design.

Heterocyclic compounds containing skeletal systems such as pyrrole, pyrazole, imidazole, thiophene, furan and indole were important raw materials in the pharmaceutical industry. Studies conducted with these heterocyclic compounds attracted the attention of the scientific world. The interest of medicinal chemists in this field has increased greatly since heterocyclic compounds play an important role in drug design. Natural and synthetic molecules containing the substituted indole analogs were known to be important due to their biological activities. Indole analogs were precursors of many pharmaceutical products. Their heterocyclic compounds have been successfully commercialized using the pharmaceutical industry [10]. The many studies revealed that analogs containing substituted indole unit in the literature were a wide variety of pharmacological activities such as anti-inflammatory, analgesic, antimicrobial, anticancer, antipyretic, antiviral, antimalarial, anti-diabetic, antidepressant [11–13].

Designed indole analogs were similar to endogenous molecules and the structure of many important biomolecules up to synthetic drug active ingredients used in a clinical pharmacology [14]. In addition, the indole-linked alkyl groups were important for antioxidant activity. It was stated in the literature that indole derivatives containing cyclohexyl, methyl, nitrogen and methoxy groups had a high free radical scavenging power [15]. In addition, 1,2,3-triazole compounds are a five-membered heterocyclic scaffold due to a wide range of biological effects such as analgesic, anti-inflammatory, antioxidant, antibacterial, antituberculosis, antifungal, anticonvulsant, and anticancer effects [16]. Furthermore, indole derivatives containing 1,2,3-triazole structure were defined as compounds with effective antioxidant activity [17]. The different substitutions having 1,2,3-triazole compounds have appeared important changes in the biological effects [18]. Indoles having 1,2,3-triazoles group was widely used in pharmaceuticals and agrochemicals [19]. As a result of the research, indole-linked alkyl groups were also significant for antioxidant activity. It was found that derivatives including cyclohexyl and methoxy groups had high free radical scavenging power [16]. During the oxidation of indole derivative compounds, an electron is removed from the nitrogen atom of the pyrrole ring and a radical cation has occurred. Due to this capacity of the pyrrole ring, the antioxidant activity of 3-substituted indole compounds is also affected by other functional groups in the molecule [20]. The synthesized indoles containing 1,2,3-triazole groups could vary according to the functional groups in their structure. This study investigated the synthesis of indole analogs resulting from the bonding of different substituents or cyclic structures to the indole structure, the bioinformatics analysis, and biological activities of the synthesized analogs on the GST and AChE. Encouraged by these successful efforts, we continue the search for the pharmacological profile of representative AChE-GST enzymes of the indoles containing 1,2,3-triazole groups by exploring heterocyclic scaffolds. Therefore, the 3-substitue 2-methyl indole analogs bearing various substituents in the 3-position were synthesized, and these analogs were carried out bioinformatics analysis and in vitro enzyme inhibition studies on AChE-GST enzymes.

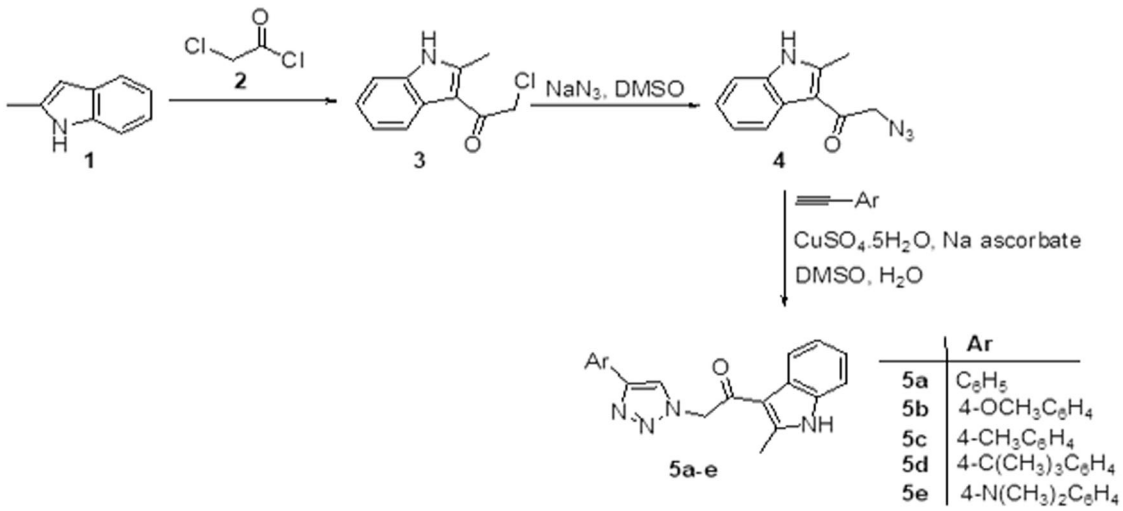

Scheme 1 Synthesis of the 3-substitue 2-methyl indole **4** and **5a-e**

Results and discussion

Synthesis of the 3-substitue 2-methyl indole analogs

Indole compounds that played an important role in skeletal system of drug design, were raw materials of the pharmaceutical industry [21]. Studies conducted with these indole-triazole compounds attracted considerable interest in their biological activities [16, 19]. The interest of medicinal chemists in synthesized indole compounds has increased greatly due to versatile indole analogs with various pharmacological activities. Therefore, indole **3** was obtained by heating 2-methyl-1*H*-indole (**1**) and 2-chloro acetyl chloride (**2**) with anhydrous toluene at boiling temperature as shown in Scheme 1. The physical properties of 3-substitue 2-methyl indole analogs (**4** and **5a**-**e**) were mentioned in retention factors (R_f), melting points and yields obtained at the end of the reaction in the experimental part. When the ^{1}H NMR spectrum of the compound is examined, the NH proton found in the indole ring was seen at δ 9.91 ppm. The protons attached to the aromatic ring in the indole structure were observed peaks in the range of δ 7.81–7.10 ppm. The H4 proton of the indole ring was observed as a doublet at δ 7.81 ppm. The H5, H6 and H7 protons were also observed as the doublet of the doublet in the range of δ 7.49–7.11 ppm. The 2H proton attached to -CH_2 showed a singlet in the range of 4.12 ppm and the 3H proton attached to -CH_3 observed a singlet at δ 2.01 ppm.

When the ^{13}C NMR spectrum was examined, it was seen that the peak of the carbonyl carbon was observed at δ 191.38 ppm, and the peak of the aromatic region carbons were observed in the range of δ 138.86–112.27 ppm. The indole **4** which is 2-azido-1-(2-methyl-1H-indol-3-yl) ethanone was obtained by reaction of the synthesized indole **3** and sodium azide in DMSO. In the ^{1}H NMR spectrum of the indole **4**, the NH proton of indole ring was observed at δ 10.15 ppm, and the protons attached to the aromatic ring were also observed the doublet of doublet in the range of δ 7.40–7.17 ppm. The 2H proton attached to CH_2 and the 3H proton bonded to CH_3 group was observed as singlet peaks at δ 2.91 and 2.01 ppm, respectively. When the ^{13}C NMR spectrum was examined, it was seen that the carbonyl carbon in the structure and the aromatic region carbons were observed at δ 191.60 ppm and in the range of δ 138.42–111.56 ppm, respectively. Furthermore, it was observed that the carbon of the methyl group in the structure was observed at a peak of δ 20.06 ppm.

The synthesized 1,2,3-triazole analogs contained different groups such as H, OCH_3, CH_3, $C(CH_3)_3$ and $N(CH_3)_2$, respectively. As seen in Scheme. 1, 1,4-substituted 1,2,3-triazole analogs **5a**-**e** were synthesized as a result of heating with indole **4**, copper sulfate pentahydrate, and acetylene derivative. When the ^{1}H NMR spectra of indole **5a** was examined; The H4 proton of the indole ring was observed as a doublet at δ 8.12 ppm with the interaction constant of *J* 8.0 Hz, and also observed the H5 proton in the 1,2,3-triazole structure as a singlet at δ 7.69 ppm. The protons of indole-H5, indole-H6, and indole-H7 were observed as the doublet of a doublet in the range of δ 7.38–7.19 ppm. In the ^{1}H NMR spectrum of indole **5a-e** compounds, NH protons in the indole ring were observed at δ 10.97–9.59 ppm. The 2H proton attached to -CH_2 and the 3H proton attached to -CH_3 showed a singlet structures at δ 4.40 ppm and δ 1.82 ppm, respectively. It was observed that the aromatic protons attached to the phenyl group observed as multiplet peaks in the range of δ 7.58–7.10 ppm. The methyl protons in the methoxy structure showed in the range of δ 1.91 ppm in ^{1}H

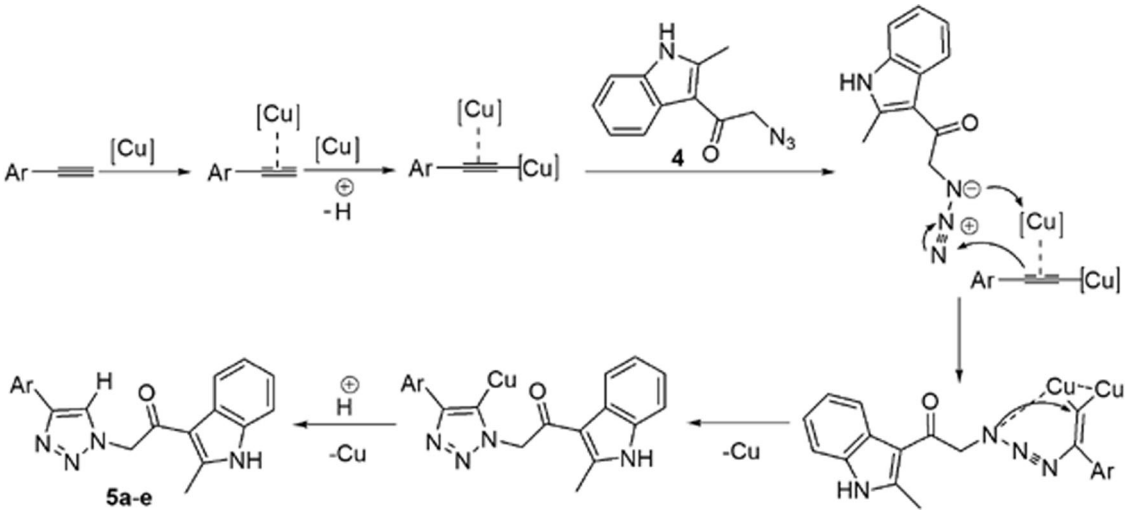

Scheme 2 Proposed mechanism for the synthesis of **5a-e**

NMR spectrum of the indole **5b** and in the ^{1}H NMR spectrum of the indole **5c** compound, the methyl group protons attached to the phenyl ring peak was observed at δ 2.57 ppm. It was also observed that the protons of the methyl groups of the phenyl-linked tertiary methyl group gave a singlet peak at δ 1.14 ppm in the ^{1}H NMR spectrum of the indole **5d**. Protons of the dimethyl group attached to the nitrogen attached to the phenyl ring were observed in the range of δ 2.88 ppm in the ^{1}H NMR spectrum of the indole **5e**. When the ^{13}C NMR spectrum was examined, it was seen the carbonyl carbon peaks in the structure at δ 191.90 ppm, and the aromatic region carbons at δ 146.10–111.51 ppm. The 1,2,3-triazole-CH carbon peak was observed at δ 146.10 ppm and the carbons attached to the phenyl group gave a peak in the range of δ 138.7–122.3. The methyl carbon peak in the methoxy structure was observed at δ 56.5 ppm in ^{13}C NMR spectrum of the indole **5b**. When the ^{13}C NMR spectrum of the indole **5c** was examined, the methyl group carbon atom attached to the phenyl group peaks observed at δ 29.3 ppm. It was observed that methyl carbon atoms in the tertiary group attached to the phenyl group observed peaks in range of δ 41.09–30.12 ppm and the carbon atom attached to the methylene group gave a peak at δ 56.61 ppm in ^{13}C NMR spectrum of the indole **5d**. It was observed that the dimethyl carbon atoms attached to the nitrogen-related phenyl structure gave a peak in the range of δ 38.90 ppm in ^{13}C NMR spectrum of the indole **5e**. The organic azides were utilized for the synthesis of the 1,4-disubstituted 1,2,3-triazoles as building blocks in medicinal chemistry [22, 23]. Copper-catalyzed azide-alkyne cycloaddition (CuAAC) was widely utilized in the most sub-disciplines of chemistry for the regioselective synthesis of the 1,4-disubstituted 1,2,3-triazoles [24, 25]. CuAAC was first reported by Meldal et al. 30 years ago. Afterwards, extensive research was carried out for CuAAC with an expanded scope of the reaction by studies of the catalyst, ligand, and solvent. A large number of mechanistic reports have been published in this field. However, the mechanism of the transformation was still difficult. Some aspects of the copper acetylide formation mechanism elucidation steps from terminal alkynes via π-coordination of copper were considered supported by computer studies and experimental studies [26]. As seen in Scheme 2, a mechanism for CuAAC cycloaddition was proposed using crossover experiments with enriched copper additives and heat flow calorimetry by Worrell et al. [27]. The reaction is formed with the formation of a sigma bond Cu acetylide and a π-coordination of a second copper(I) ion. Triazole structure has occurred with dipolar cycloaddition and the azide complexation. The indole-triazole analogs **5a-e** were released with protonation, and the copper catalyst becomes free.

Enzyme inhibitory properties of the substituted indole analogs

The need for suitable tool analogs for pharmacological studies of brain diseases and especially, the good inhibitors for AD led to the initiation of these enzymes studies. Enzyme inhibitory experiments with indole-triazole analogs were proven to be a valuable tool in the new drug research. The 3-substitue 2-methyl indole analogs have enabled researchers to identify AChE and GST targets. The most important aim of the inhibitor study has been to carry out similar molecular structures to existing drugs in drug discovery. Therefore, the biological studies were to identify potent and selective inhibitors for AChE and GST. Since the structure of 3-substituted 2-methyl indole analogs were

Table 1 AChE and GSTs inhibition activities of the 3-substitue 2-methyl indole analogs

Indole	IC_{50} (μM)				Ki (μM)	
	AChE	R^2	GST	R^2	AChE	GST
4	0.55	0.904	1.58	0.977	0.75 ± 0.35	0.79 ± 0.35
5a	3.06	0.984	3.74	0.982	4.36 ± 0.76	2.78 ± 0.67
5b	2.37	0.988	2.95	0.982	3.15 ± 1.20	5.05 ± 1.02
5c	0.63	0.995	0.60	0.998	1.18 ± 0.26	1.48 ± 0.49
5d	3.57	0.950	4.62	0.986	3.39 ± 0.73	6.70 ± 2.19
5e	2.67	0.986	3.43	0.976	7.29 ± 5.95	2.88 ± 0.89
Tacrine*	0.848	0.996	-	-	0.556	-
Ethacrynic acid*	-	-	0.374	0.9632		0.386

*Standard inhibitors for the ACHE and GST enzymes

close to the standard inhibitors used in brain diseases, these heterocyclic compounds were designed in this study [10, 21]. The synthesized 3-substitue 2-methyl indole analogs were applied on AChE and GST targets, and also were used to obtain binding sites. The inhibition study was carried out for both enzymes in two steps, IC_{50} and Ki. The IC_{50} values for the AChE enzyme of 3-substitue 2-methyl indole analogs were determined in the range of 0.55–2.67. Tacrine molecule, which is widely used as a standard inhibitor of the AChE enzyme, was also used in the study. IC_{50} and R^2 values were found to be 1.65 and 0.977 respectively. In addition to, the Ki study was done. Ki values were found between 0.75 ± 0.35-7.29 ± 5.95 for this enzyme. To compare the effectiveness of the results, a Ki study was performed for the standard inhibitor Tacrine, and the Ki value of the Tacrine molecule was found to be 0.99 ± 0.26. The biological results of all analogs are depicted in Table 1. After examination of the results, it was seen that the indole **4** analog showed better inhibition than the standard inhibitor for AChE. When the studies done by the authors were examined, there were similar results in the literature [10]. When the results of glutathione S-transferase enzyme inhibition study of molecules were examined, IC_{50} values were found between 0.6–3.74 respectively. Ethacrynic acid standard was used in GST enzyme and IC_{50}, R^2 values were found as 0.77 and 0.996, respectively. Ki results were found to be 0.79 ± 0.35–6.70 ± 2.19 and standard inhibitor Ki values 0.81 ± 0.31, respectively. The indole **4** analog was seen that the effect of inhibitors on the GST enzyme is lower than the standard. When the studies done by the authors were examined, there were similar results in the literature [28, 29].

The previously suggested cation-π interactions between the substitutions of arginine amino acid to AChE, were addressed with the synthesis of the functional moieties and heterocyclic moieties-containing indole-triazole analogs. A decreasing affinity with an increasing number of the functional phenyl, methyl, *tert*-buthyl, methoxy, and azide moieties could have indicated the presence of a cation-π interaction. Still, no significant alterations in the binding affinities for neither the AChE binding sites nor the GST binding site were displayed [10]. Generally, it seemed that recognition of the AChE binding site was more affected by the nature of the substituents than the electron density of the heterocyclic structures. The study showed that the SAR's of the synthesized 3-substitue 2-methyl indole analogs and the high-affinity GSTs binding sites were different. The GSTs receptor binding affinity of synthesized 3-substitue 2-methyl indole analogs was also confirmed. Since all the indole-triazole analogs showed some degree of affinity towards both binding sites, no highly selective GSTs analogs were found in this series of 3-substitue 2-methyl indole analogs. These synthesized 3-substituted 2-methyl indole analogs have emerged as potential precursors for AChE and GST in terms of their biological properties. It is thought that these synthesized indole-triazole analogs might be important in various fields such as active pharmaceutical ingredients and catalysts.

Molecular docking studies

Lead drug discovery of the indole analogs was widely utilized as anti-inflammatory, anti-angiogenic, and antioxidant activities [30–32]. The binding affinities, hydrogen bonds and bond lengths were obtained using Autodock Vina between the AChE-GST enzymes and indole analogs. The natural ligand as reference ligand, Tacrine and Ethacrynic acid as a standard drug were used to compare molecular docking results of the indole analogs. Synthesized indole-triazole analogs were investigated as potential inhibitors of the AChE-GST enzymes. All indole analogs were inserted using optimized molecular docking conditions into the active sites of the AChE-GST enzymes. The binding energy, inhibition activity, ligand activity, and hydrophobic, hydrogen bonds, and electrostatic interactions of the indole analogs and AChE-GST enzymes' complexes were depicted in Table 2.

Table 2 The binding affinity, ligand efficiency, and inhibition activity values of the 3-substitue 2-methyl indole analogs into the active catalytic pocket of the AChE and GSTs enzymes

Indole	AChE		GST			
	Binding Affinity (kcal/mol)	Ligand Efficiency	Inhibition Activity (uM)	Binding Affinity (kcal/mol)	Ligand Efficiency	Inhibition Activity (uM)
4	−6.0	−0.54	43.14	−7.5	0.47	3.29
5a	−9.3	−0.39	167.23	−9.3	−0.39	0.154
5b	−8.3	−0.32	863.87	−9.8	−0.38	0.062
5c	−8.9	−0.34	281.88	−9.8	−0.39	0.062
5d	−8.6	−0.31	472.39	−11.1	−0.40	0.007
5e	−9.0	−0.33	268.89	−9.9	−0.37	0.060
Tacrine*	−6.4	−0.43	20.63		-	-
Ethacrynic acid**	-	-		−7.7	−0.59	5.58

Standard inhibitors for the ACHE* and GST* enzymes

**TAC and Ethacrynic acid were used as reference drugs for the AChE and GST

Drug scores, Volume Å^3, and Surface Å^3 were determined for indole analogs-AChE and GST enzyme 0.83, 912.16 and 1088.06, respectively. The crystal poses of the synthesized indole analogs were placed with defined search algorithms and scoring functions in the binding site of the AChE-GST enzymes. The ligand efficiencies of the indoles-AChE complexes' were obtained between −0.39 and −0.31. Binding affinity values of the indoles-AChE complexes' were found between −9.3 and −8.3 kcal/mol. The binding affinities of all indole-AChE complexes' were found to be higher than the reference ligand value for AChE. The binding affinity of indole **5a-**AChE complex was found as −9.3 kcal/mol. The binding affinity of indole **5e-**AChE complex was very close value of −9.0 kcal/mol and the binding affinity of indole **5b-**AChE complex was found to be lower value of −8.3 kcal/mol than other indole ligands. This is thought to be due to the triazole, phenyl, and different structures of the substituted indole analogs [33, 34]. When the molecular docking results of all indole-AChE complexes' were examined, all complexes showed alkyl interactions with amino acid residues Lys332, Ala528, His381, Val330, Val408, Ala526, Ala525, Arg525, Tyr382 in the active site of the AChE in Table 3. All complexes showed π-alkyl interactions with amino acid residues Val330, Val408, Ala526, Ala528, Arg525, Lys332, Ala518, Leu524, and Val429 in the active site of the AChE. All indole-AChE complexes' except indole **5a** and **5b**-AChE complexes showed a Van der Waals interaction with the amino acid residues Val331, Glu431, Arg522, His381, Ala526, Gly523, Asp404, and Asp400 in the active site of the AChE. As shown in Fig. 1, the complex structures between indole analogs and AChE were stabilized simultaneously as donor and acceptor with hydrogen bonds containing oxygen (-O), hydrogen (-H), nitrogen (-N), indole, triazole, and carbonyl (-C = O) moieties and Cys145, Leu141, Glu166, Arg188, Thr190, Asn142, Gly143, Ser144, His163, Asp148, His164, Gln189, Pro168. All complexes showed π donor hydrogen bonds, π-sigma, and π-cation electronic interactions with amino acid residues Arg525 and Val429 in the active site of AChE. Also, indole **5c**-AChE complexes showed π-π T-shaped electronic interaction with amino acid residue Tyr510 in the active site of AChE. In addition, binding affinity values of the indole-GST complexes' were found between −11.1 and −7.5 kcal/mol.

The binding affinities of indole (**5a-e**)-GST complexes' were found to be higher than the reference ligand value for GST. The binding affinity of the indole **5d-**GST complex was found as −11.1 kcal/mol. The binding affinity of indole **5e-**AChE complex was very close value of −9.9 kcal/mol and the binding affinity of indole **5b-**AChE complex was found to be lower value of −9.3 kcal/mol than other indole ligands. When the molecular docking results of all indole-AChE complexes' were examined, all complexes showed alkyl and π-alkyl interactions with amino acid residues Cys63, Cys58, Ala342, Ala 155, Ile198, and Lys66 in the active site of the GST. The all indole (**5a-e**)-GST complexes' were stabilized simultaneously as donors and acceptors with hydrogen bonds containing oxygen, hydrogen, nitrogen, indole, triazole, carbonyl moieties and Ser30, Thr57, Lys66, Pro340, Ala155, Cys63, Glu201 as shown in Table 3.

All indole (**5a-e**)-GST complexes' showed a π-donor H bond interaction with the amino acid residues Tyr197 and Asp331 in the active site of the GST. All indole (**5a-e**)-GST complexes' (except indole **5a**-GST complex) showed a π anion electronic interaction with the amino acid residue Asp331 in the active site of the GST. However, the indole **5a**-GST complex just showed a π-cation electronic interaction with the amino acid residue Thr369 in the active site of the GST. Furthermore, the indole **5d**-GST complex also showed a π-sulphur electronic interaction with the amino acid residue Met202 in the active site of the GST. All

Table 3 Molecular interactions of the AChE and GST active sites with the 3-substitue 2-methyl indole analogs

Complex	Type of interactions	Interacting residues
AChE-4	H-bond, π-cation, π-donor H bond, π-sigma, alkyl, π-alkyl	Gly523, Tyr510, Arg521, Lys332, Arg525, Val429, Val330, Val408
AChE-5a	H-bond, π-cation, π-donor H bond, π-sigma, alkyl, π-alkyl	Arg525, Arg521, Tyr510, Lys332, Val330
AChE-5b	H-bond, π-cation, π-donor H bond, π-sigma, alkyl, π-alkyl	Arg525, Arg521, Tyr510, Val429, Ala528, His381, Lys332, Val330
AChE-5c	H-bond, π-cation, π-donor H bond, π-sigma, π-π T shaped, Van Der Waals, alkyl, π-alkyl	Arg525, Arg521, Tyr510, Val429, Arg526, Val331, Glu431, Arg522, Val308, Val330, Lys332
AChE-5d	H-bond, π-cation, π-donor H bond, π-sigma, Van Der Waals, alkyl, π-alkyl	Arg525, Arg521, Tyr510, Val429, Arg525, His381, Asp430, Ala526, Gly523, Lys332, Tyr382, Ala528, Ala518, Val408, Val330,
AChE-5e	H-bond, π-cation, π-donor H bond, π-sigma, π-cation, π-anion, Van Der Waals, alkyl, π-alkyl	Arg525, Arg521, Tyr510, Ala526, Gln527, Lys332, Glu431, Val429, Gly523, Arg522, Val331, Val408, Val330,
GST-4	H-bond, π-anion, alkyl, π-alkyl	Ser30, Thr57, Cys58, Ala155, Asp331, Cys63, Ala342
GST-5a	H-bond, π-cation, π-donor H bond, π-sigma, alkyl, π-alkyl	Lys66, Pro340, Tyr 197, Thr369, Val370, Leu338, Cys63, Ile198
GST-5b	H-bond, π-anion, π-donor H bond, π-sigma, alkyl, π-alkyl	Cys63, Glu201, Ala155, Asp331, Tyr197, Gly62, Ile198, Ala342, Lys66
GST-5c	H-bond, π-anion, π-donor H bond, alkyl, π-alkyl	Cys63, Glu201, Asp331, Tyr197, Ile198, Ala342, Lys66
GST-5d	H-bond, π-anion, π-donor H bond, π-sulphur, alkyl, π-alkyl	Cys63, Glu201, Asp331, Tyr197, Met202, Ile198, Ala342, Lys66
GST-5e	H-bond, π-anion, π-donor H bond, π-sigma, alkyl, π-alkyl	Cys63, Glu201, Asp331, Tyr197, Val329, Ala155, Ile198, Cys58, Ala342, Lys66

indole-GST complexes' (except indole **5a** and **5d**-GST complex) showed a π-sigma electronic interaction with the amino acid residues Leu338, Gly62, and Ile198 in the active site of the GST.

Pharmacokinetic studies

All molecules are likely to diffuse, absorb or transport easily due to the low molecular weights of synthesized indole-triazoles. The cLogP (oil soluble) values of the molecules were found to range between 2.20 and −3.03. Log S (water-soluble) values of the molecules also varied range between −3.27 and −5.54. The TPSA values of the synthesized compounds were 72.80–63.57 Å2. These results could also indicate a good intestinal absorption. The pharmacokinetics of all compounds was predicted to have good gastrointestinal (GI) absorption. The ADME properties of the synthesized compounds were investigated using the Osiris, Molinspiration and SwissADME web tools as shown Table 4 [35]. A drug candidate needs to have good pharmacological activity, as well as comply with the range of values for absorption, distribution, metabolism, and excretion (ADME), and the Lipinski rule. It was observed that all synthesized indole-triazole analogs obeyed the Lipinski rule. It has been determined that synthesized compounds containing indole-triazole analogs were more likely to be drug candidates, and the tertiary group (-$C(CH_3)_3$) attached to the phenyl ring in the structure which is the **5d** analogue had the best bioavailability feature.

Conclusions

Syntheses of novel heterocyclic analogs based on the privileged indole scaffold were developed. In vitro studies revealed that indole analogs **4** and **5c** displayed binding affinity in the low micromolar range ($Ki \pm SEM = 0.75 \pm 0.35\ \mu M$ and $1.18 \pm 0.26\ \mu M$) at AChE. In addition, indole analogs **4** and **5c** displayed binding affinity in the low micromolar range at GST ($Ki \pm SEM = 0.79 \pm 0.35\ \mu M$ and $1.48 \pm 0.49\ \mu M$). Indole **4** was evaluated the best inhibitory activity against AChE, and GST enzymes with the lowest IC_{50} values as 0.55 μM and 1.58 μM, respectively. Furthermore, indole **5c** exhibited significant activity at GST ($IC_{50} = 0.60\ \mu M$), and AChE with a low IC_{50} value as 0.63 μM. In addition, the molecular interaction analyses and molecular docking properties of AChE and GST-indole analogs' complexes revealed to show similar binding conformations. The binding affinities of the AChE-**5a** and **5e** analogs' complexes were found to be −9.3 and 9.0 (kcal/mol) with the residues of Arg525, Arg521, Tyr510, Ala526, Gln527 and Glu431. Also, the binding affinities of GST-**5d** analog' complex was found to be −11.1 (kcal/mol) with the residues of Cys63, Glu201, Asp331, Tyr19, and Met202. A stable conformer and good binding site of the

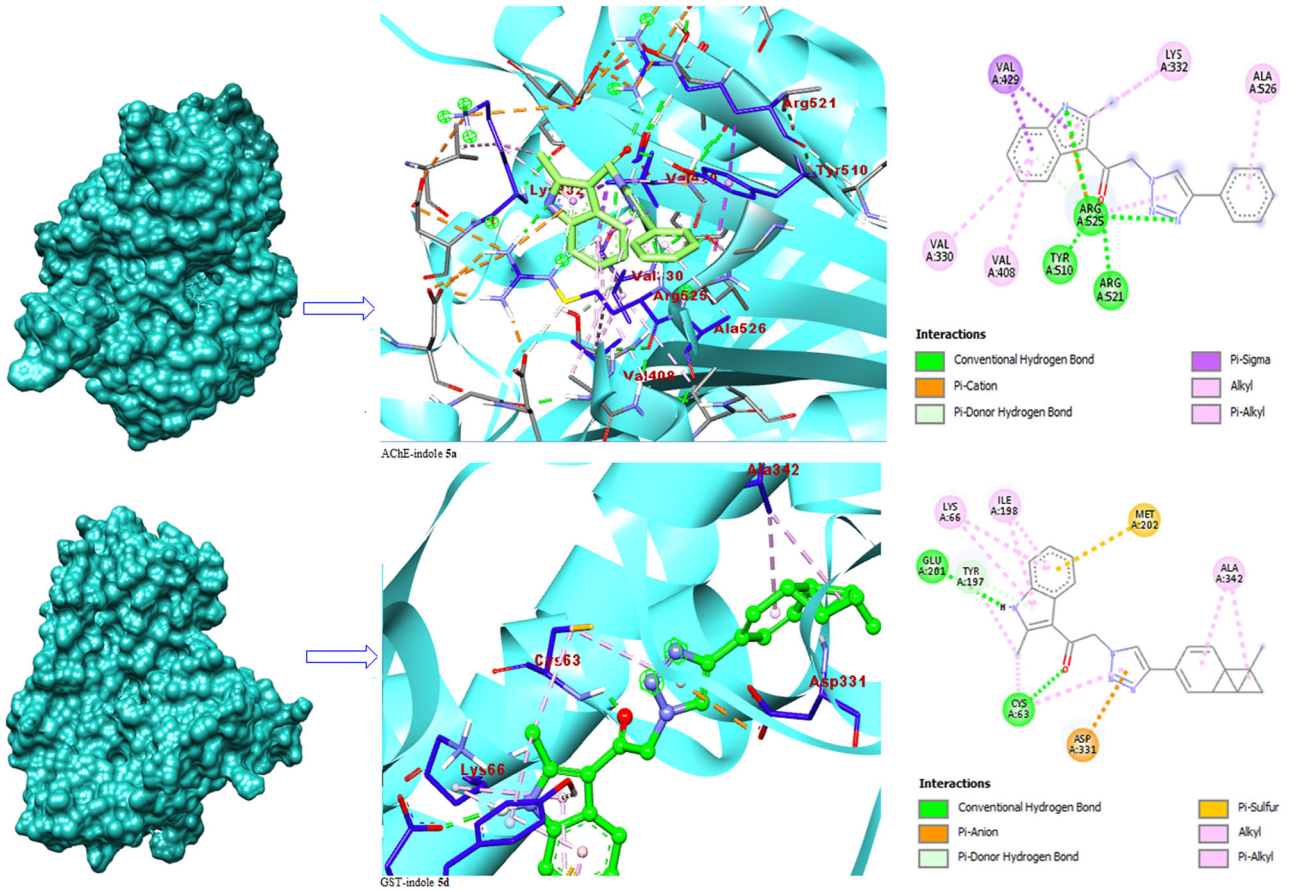

Fig. 1 The 2D and 3D interaction diagram of enzymes and indole compounds. AChE (PDB ID:4M0E)-indole 5a, GST (PDB ID:3DK9)-indole 5d

3-substitue 2-methyl indole analogs occurred by creating aromatic, hydrogen, and hydrophobic bonds in the AChE and GST active site residues. It was observed that 3-substitue 2-methyl indole analogs could be strong inhibitor candidates. Moreover, when the inhibition results are examined, we can recommend the use of 3-substitue 2-methyl indole analog **4** as a standard inhibitor after in vivo testing.

Experimental

General

All chemicals were purchased from Merck and Sigma–Aldrich companies. All reagents and solvents were utilized without further purification. The development of reactions was monitored by thin layer chromatography (TLC) analysis on Merck pre-coated silica gel 60 F254 aluminum sheets, visualized by UV light. Melting points were recorded on an Electrothermal Gallenkamp apparatus and are uncorrected. HPLC was performed on the Shimadzu LC-20 system (Shimadzu, Japan) and a diode array detector SPD-M20A (190–800 nm) was utilized. ^{1}H and ^{13}C NMR spectra were recorded on a Varian Mercury-400 High-performance Digital FT-NMR Spectrophotometer (*Varian*, Fort Collins, CO, USA) at 400 MHz and 100 MHz, respectively. During the measurements, tetramethylsilane (TMS) was used as an internal standard and deuterated $CDCl_3$ as the solvent. The chemical shifts are reported in parts per million (ppm, δ) downfield from the TMS. The following abbreviations are used; singlet (s), doublet (d), triplet (t), quartet (q), multiplet (m), and broad (br s). The mass spectra were taken with Thermo Scientific TSQ-Quantum Access LC/MS spectrometers. The following software was performed in the present study: (i) AutoDock 4.2.6, (ii) MGLTools 1.5.6, (iii) Babel-2.4.0, (iv) BIOVIA Discovery Studio 4.5, (v) Chemdraw Ultra 8.0, (vi) Java Platform, (vii) The utilized online web tools: -http://www.swissadme.ch, -http://www.molinspiration.com/cgi-bin/properties, -https://www.organic-chemistry.org/prog/peo/

2-chloro-1-(2-methyl-1H-indol-3-yl)ethanone (3)

The title indole analog was prepared from a published procedure [36]. $R_f = 0.30$ (40% EtOAc in n-heptane, v/v). M.p: (°C): 212-214; ^{1}H NMR (400 MHz, $CDCl_3$): δ 9.91 (*br s*, 1H, NH), 7.81 (*d*, J = 8.0 Hz, 1H, indol-H4), 7.49

Table 4 Drug likeliness properties of the 3-substitue 2-methyl indole analogs by some web tools[a,b,c]

Drug likeness properties	5a	5a	5c	5d	5e	Tacrine	Ethacrynic acid
Bioavailability and drug-score[a]							
Molecular weight g/mol	316.36	346.38	330.38	372.46	359.42	198.26	302.0
cLogP	2.20	2.47	2.48	3.03	2.54	2.09	3.13
Log S	−4.29	−4.34	−4.58	−5.54	−4.50	−3.27	−4.17
TPSA (Å²)	63.57	72.80	63.57	63.57	66.81	38.91	63.6
Druglikeness	0.37	0.43	−0.86	−3.0	−0.72	−7.18	−2.84
Drug-score	0.55	0.6	0.46	0.29	0.29	0.16	0.14
Toxicity risks[a]							
Mutagenic	nt	nt	nt	nt	nt	ht	nt
Tumorigenic	nt	nt	nt	nt	ht	ht	nt
Irritant	nt	nt	nt	nt	nt	nt	Ht
Reproductive effective	nt	nt	nt	nt	nt	nt	ht
Druglikeness[b]							
GPCR ligand	0.23	0.17	0.19	0.23	0.20	−0.11	−0.30
Ion channel modulator	−0.29	−034	−0.34	−0.20	−0.29	0.36	−0.34
Kinase inhibitor	0.10	0.06	0.06	0.08	0.12	−0.37	−0.66
Nuclear receptor ligand	−0.60	−0.57	−0.61	−0.42	−0.54	−0.93	0.33
Protease inhibitors	−0.12	−0.16	−0.15	−0.10	−0.13	−0.59	−0.72
Enzyme inhibitor	0.24	0.17	0.18	0.21	0.19	0.43	0.02
Pharmacokinetics[c]							
BBB permeant	yes	yes	yes	yes	yes	yes	yes
GI absorption	high	high	high	high	high	high	high
P-gp	no	no	no	yes	no	yes	no
1A2	yes	yes	yes	yes	yes	yes	yes
2C19	yes	yes	yes	yes	yes	no	yes
2C9	yes	yes	yes	yes	yes	no	no
2D6	yes	yes	yes	no	yes	no	no
3A4	yes	yes	yes	yes	yes	yes	no

nt not toxic, *ht* high toxic, *GI* gastrointestinal absorption, *BBB* blood brain barrier, *P-gp* permeability glycoprotein, *CYP* cytochrome P450

[a]Osiris

[b]Molinspiration

[c]SwissAdme

(*ddd*, J = 8.0, 1.2, 0.9 Hz, 1H, indol-H7), 7.25 (*ddd*, J = 8.2, 7.6, 1.4 Hz, 1H, indol-H6), 7.11 (*ddd*, J = 8.4, 7.2, 1.0 Hz, 1H, indol-H5), 4.12 (*s*, 2H, CH_2), 2.01 (*s*, 3H, CH_3). ^{13}C NMR (100 MHz, $CDCI_3$): δ 191.3 (CO), 138.8 (indole-C7a), 131.9 (indole-C2), 128.9 (indole-C3a), 128.6 (indole-C6), 127.7 (indole-C5), 123.4 (indole-C4), 120.4 (indole-C3), 112.2 (indole-C7), 41.08 (CH_2), 21.0 (CH_3).

2-azido-1-(2-methyl-1H-indol-3-yl)ethanone (4)

Indole **3** (0.103 g, 0.5 mmol) was dissolved in DMSO (2 mL). Sodium azide (0.05 g, 0.75 mmol) was added to the solution. The reaction process was stirred at −5 °C for 30 min. Then, it was heated until room temperature for 3 h. H_2O (10 mL) was added, the aqueous phase was extracted with diethyl ether (3 × 20 mL) and the combined organic phases were washed with water (3 × 20 mL). The solvent was dried over Na_2SO_4, removed under reduced pressure and the crude product was purified by silica gel flash column using ethylacetate:heptane (1:6) as the eluent. White solid (0.15 g, 58%), R_f = 0.35 (n-hexane %30 EtOAc, v/v); M.p (°C): 132–134; Purity: 98.27% (HPLC); ^1H NMR (400 MHz, $CDCI_3$): δ 10.15 (*br s*, 1H, NH), 7.40 (*d*, J = 8.0 Hz, 1H, indole-H4), 7.38 (*ddd*, J = 8.0, 1.2, 0.9 Hz, 1H, indole-H7), 7.28 (*ddd*, J = 8.2, 7.6, 1.4 Hz, 1H, indole-H6), 7.17 (*ddd*, J = 8.4, 7.2, 1.0 Hz, 1H, indole-H5), 2.91 (*s*, 2H, CH_2), 2.01 (*s*, 3H, CH_3). ^{13}C NMR (100 MHz, $CDCI_3$): δ 191.6 (C = O), 138.4 (indole-C7a), 133.1 (indole-C2), 129.3 (indole-C3a), 128.2 (indole-C6), 127.5 (indole-C5), 122.8 (indole-C4), 119.4 (indole-C3), 111.5 (indole-C7), 51.0 (-CH_2), 20.0 (-CH_3).

General procedure for indole-triazole synthesis (5a-e)

Indole **4** (0.12 g, 0.5 mmol) was added in DMSO (4 mL) and H_2O (0.5 mL). Copper(II) sulfate pentahydrate (0.0063 g, 0.025 mmol) and sodium ascorbate (0.01 g, 0.05 mmol) were added in solution. Then the acetylene derivatives (1-ethynyl benzene, 1-ethynyl-4-methyl benzene, 1-ethynyl-4-methoxybenzene, 4-ethynyl-*N*,*N*-dimethylbenzenamine, 1-*tert*-butyl-4-ethynylbenzene) were added in solution. Reaction process was stirred for 3 h at room temperature. H_2O (30 mL)was added, the aqueous phase was extracted with diethyl ether (3 × 15 mL) and the combined organic phases were washed with water (3 × 15 mL). The solvent was dried over Na_2SO_4, removed under reduced pressure and the crude product was purified by silica gel flash column using ethylacetate:heptane (1:7) as the eluent.

1-(2-methyl-1H-indol-3-yl)-2-(4-phenyl-1H-1,2,3-triazol-1-yl)ethanone (5a)

Yield: %74; $R_f = 0.40$ (n-hexane %40 EtOAc, v/v); M.p (°C): 148-150; Purity: 96.08% (HPLC); ^{1}H NMR (400 MHz, $CDCl_3$): δ 10.97 (*br s*, 1H, NH), 8.12 (*d*, J = 8.0 Hz, 1H, indole-H4), 7.69 (*s*, 1H, triazole-H5), 7.58–7.10 (*m*, 5H, PhH), 7.38 (*ddd*, J = 8.0, 1.2, 0.9 Hz, 1H, indole-H7), 7.28 (*ddd*, J = 8.2, 7.6, 1.4 Hz, 1H, indole-H6), 7.19 (*ddd*, J = 8.4, 7.2, 1.0 Hz, 1H, indole-H5), 4.40 (*s*, 2H, CH_2), 1.82 (*s*, 3H, CH_3). ^{13}C NMR (100 MHz, $CDCl_3$): δ 191.9 (C = O), 146.1 (triazole-C4), 139.4 (indole-C7a), 131.0 (indole-C2), 138.7–122.3 (Ph-CH), 130.4 (triazole-CH), 128.0 (indole-C3a), 125.7 (indole-C6), 124.4 (indole-C5), 120.4 (indole-C4), 119.0 (indole-C3), 111.5 (indole-C7), 55.6 (-CH_2), 18.6 (-CH_3). LC/MS: (ESI) $[M + H]^+$: $C_{19}H_{16}N_4O$: Calcd. for 317.1402; found 317.1399.

2-(4-(4-methoxyphenyl)-1H-1,2,3-triazol-1-yl)-1-(2-methyl-1H-indol-3-yl)ethanone (5b)

Yield: %70; $R_f = 0.36$ (n-hexane %40 EtOAc, v/v); M.p (°C): 168–170.5; Purity: 97.07% (HPLC); ^{1}H NMR (400 MHz, $CDCl_3$): δ 9.95 (*br s*, 1H, NH), 8.04 (*d*, J = 8.0 Hz, 1H, indole-H4), 7.87 (*s*, 1H, triazole-H5), 7.59–6.99 (*m*, 4H, PhH), 7.45 (*ddd*, J = 8.0, 1.2, 0.9 Hz, 1H, indole-H7), 7.30 (*ddd*, J = 8.2, 7.6, 1.4 Hz, 1H, indole-H6), 7.19 (*ddd*, J = 8.4, 7.2, 1.0 Hz, 1H, indole-H5), 4.63 (*s*, 2H, CH_2), 3.32 (*s*, 3H, CH_3), 1.91 (*s*, 3H, CH_3). ^{13}C NMR (100 MHz, $CDCl_3$): δ 191.2 (C = O), 162.7 (Ph-C), 146.8 (triazole-C4), 140.7 (indole-C7a), 131.9 (indole-C2), 137.5-121.1 (5xPh) -CH), 130.3 (triazole-CH), 128.7 (indole-C3a), 124.8 (indole-C6), 123.2 (indole-C5), 120.5 (indole-C4), 119.1 (indole-C3), 111.2 (indole-C7), 56.5 (-OCH_3), 49.6 (-CH_2), 18.6 (-CH_3). LC/MS: (ESI) $[M + H]^+$: $C_{20}H_{18}N_4O_2$: Calcd. for 347.1508; found 347.1503.

1-(2-methyl-1H-indol-3-yl)-2-(4-p-tolyl-1H-1,2,3-triazol-1-yl)ethanone (5c)

Yield: %68; $R_f = 0.35$ (n-hexane %40 EtOAc, v/v); M.p (°C): 155-157; Purity: 98.25% (HPLC); ^{1}H NMR (400 MHz, $CDCl_3$): δ 10.49 (*br s*, 1H, NH), 7.72 (*d*, J = 8.0 Hz, 1H, indole-H4), 7.71 (*s*, 1H, triazole-H5), 7.58–7.12 (*m*, 4H, PhH), 7.47 (*ddd*, J = 8.0, 1.2, 0.9 Hz, 1H, indole-H7), 7.28 (*ddd*, J = 8.2, 7.6, 1.4 Hz, 1H, indole-H6), 7.16 (*ddd*, J = 8.4, 7.2, 1.0 Hz, 1H, indole-H5), 3.97 (*s*, 2H, CH_2), 2.57 (*s*, 3H, CH_3), 2.26 (*s*, 3H, CH_3). ^{13}C NMR (100 MHz, $CDCl_3$): δ 192.0 (C = O), 147.0 (triazole-C4), 139.4 (Ph-C), 131.5 (indole-C7a), 130.6 (indole-C2), 128.3-123.2 (5xPh) -CH), 127.9 (triazole-CH), 127.2 (indole-C3a), 122.2 (indole-C6), 121.0 (indole-C5), 120.5 (indole-C4), 113.5 (indole-C3), 111.0 (indole-C7), 58.2 (-CH_2), 29.3, 20.6 (-CH_3). LC/MS: (ESI) $[M + H]^+$: $C_{20}H_{18}N_4O$: Calcd. for 331.1558; found 331.1554.

2-(4-(4-tert-butylphenyl)-1H-1,2,3-triazol-1-yl)-1-(2-methyl-1H-indol-3-yl)ethanone (5d)

Yield: %65; $R_f = 0.30$ (n-hexane %40 EtOAc, v/v); M.p (°C): 141–143; Purity: 96.93% (HPLC); ^{1}H NMR (400 MHz, $CDCl_3$): δ 9.59 (*br s*, 1H, NH), 7.50 (*d*, J = 8.0 Hz, 1H, indole-H4), 7.48 (*s*, 1H, triazole-H5), 7.30–6.73 (*m*, 4H, PhH), 7.29 (*ddd*, J = 8.0, 1.2, 0.9 Hz, 1H, indole-H7), 7.19 (*ddd*, J = 8.2, 7.6, 1.4 Hz, 1H, indole-H6), 6.96 (*ddd*, J = 8.4, 7.2, 1.0 Hz, 1H, indole-H5), 4.78 (*s*, 2H, CH_2), 1.97 (*s*, 3H, CH_3), 1.14 (*s*, 9H, CH_3). ^{13}C NMR (100 MHz, $CDCl_3$) δ 191.7 (C = O), 149.4 (triazole-C4), 141.8 (Ph-C), 140.0 (indole-C7a), 132.8 (indole-C2), 130.8–108.9 (5xPh) -CH), 129.8 (triazole-CH), 128.1 (indole-C3a), 125.6 (indole-C6) 123.5 (indole-C5), 122.2 (indole-C4), 113.8 (indole-C3),111.9 (indole-C7) 56.6 (-CH_2), 41.0 (-C), 30.1, 11.6 (-CH_3). $C_{23}H_{24}N_4O$: Calcd. for 373.2028; found 373.2023.

2-(4-(4-(dimethylamino)phenyl)-1H-1,2,3-triazol-1-yl)-1-(2-methyl-1H-indol-3-yl)ethanone (5e)

Yield: %58; $R_f = 0.30$ (n-hexane %30 EtOAc, v/v); M.p (°C): 151–152.5; Purity: 97.34% (HPLC); ^{1}H NMR (400 MHz, $CDCl_3$): δ 10.24 (*br s*, 1H, NH), 7.90 (*d*, J = 8.0 Hz, 1H, indole-H4), 7.67 (*s*, 1H, triazole-H5), 7.44–6.54 (*m*, 4H, PhH), 7.30 (*ddd*, J = 8.0, 1.2, 0.9 Hz, 1H, indole-H7), 7.19 (*ddd*, J = 8.2, 7.6, 1.4 Hz, 1H, indole-H6), 6.86 (*ddd*, J = 8.4, 7.2, 1.0 Hz, 1H, indole-H5), 5.23 (*s*, 2H, CH_2), 2.88 (*s*, 6H, CH_3), 2.39 (*s*, 3H, CH_3). ^{13}C NMR (100 MHz, $CDCl_3$): δ 191.5 (C = O), 150.1 (triazole-C4), 141.4 (Ph-C), 132.0 (indole-C7a), 129.3 (indole-C2), 129.0–107.7 ((5xPh) -CH), 127.3 (triazole-CH), 124.6 (indole-C3a), 123.6 (indole-C6), 121.9 (indole-C5), 119.2

(indole-C4), 116.5 (indole-C3), 111.1 (indole-C7), 56.0 (-CH_2), 38.9, 13.9 (-CH_3). LC/MS: (ESI) $[M+H]^+$: $C_{21}H_{21}N_5O$: Calcd. for 360.1824; found 360.1820.

AChE activity methods

The AChE inhibitory activity was determined by using electric eel AChE. It was purchased from Sigma. The AChE inhibition assays were carried out according to Ellman et al. method (1961) [37]. Acetyl thiocholine (ATChI) iodide was employed as the substrate of the reactions. 5,5-Dithiobis(2-nitrobenzioc) acid (DTNB) was used for the measurement of AChE activity. The hydrolysis of the substrate was monitored spectrophotometrically at a wavelength of 412 nm.

GST activity methods

The GST inhibitory activity was determined by using equine liver. The enzyme was purchased from Sigma (G6511). The GST inhibition assays were carried out according to Habig et al. method (1974) [38].

Ligand preparation

The indole-triazole analogs were used for the molecular docking study. 3D structures of the 3-substitue 2-methyl indole analogs were drawn with Chemdraw Ultra 8.0 software. The 3D structures of the 3-substitue 2-methyl indole analogs were saved in sdf format. The utilized files for molecular docking were converted in pdb format using Babel-2.4.0 software and energy minimization of the 3-substitue 2-methyl indole analogs was carried out by the Avogadro software. And hydrogen bonds in the 3-substitue 2-methyl indole analogs were added. The assigned rotatable bonds and Gasteiger charges using Autodock 4.2.6 software and then the 3-substitue 2-methyl indole analogs were saved in pdbqt for further docking processes [39].

Protein preparation

The three-dimensional x-ray crystal structure of AChE (pdb code: 4M0E, 2.00 Å) and GST (pdb code: 3DK9, 0.95 Å) enzymes were retrieved in pdb format from Protein Data Bank. The structures of selected enzymes in complex with an inhibitor were prepared by using Autodock 4.2.6 software. The complex structure between the enzymes and co-crystallized inhibitors of the AChE and GSTs was illustrated by the Autodock 4.2.6 software [40].

Molecular docking

Autodock Vina program was performed between the 3-substitue 2-methyl indole analogs and AChE/GST enzymes for molecular docking analysis such as binding types, binding energies, inhibition activities, ligand efficiency, distances, and possible interactions. Their molecular docking scores were set as Autodock 4.2.6 tools and BIOVIA Discovery Studio software of the molecular graphics laboratory software package by keeping the analog flexible [28]. The grid box center were adjusted (X = 9.239, Y = −59.985 and Z = 25.538 for AChE) and (X = 16.807 Y = 17.303 and Z = 20.702 for GSTs) with dimensions for the enzymes. The grid maps were performed with 40 × 40 × 40 points in the active sites of the AChE and GSTs enzymes and a grid-point spacing of 0.5 Å. The parameters used were 50 runs and a population size of 300. The docking protocol has validated using re-docking of co-crystallized molecule back into used the same active binding site of the AChE/GST enzymes, and it was observed interaction patterns of the AChE/GST-3-substitue 2-methyl indole analogs' complexes. The docking study was performed docking of co-crystal ligand against the generated grid showing exactly the same docking mode and in this way, the used protocol was validated by the generated grid. After validation of the docking protocol, binding conformations of the 3-substitue 2-methyl indole analogs based on virtual screening into the active sites of AChE/GST enzymes in Fig. 2.

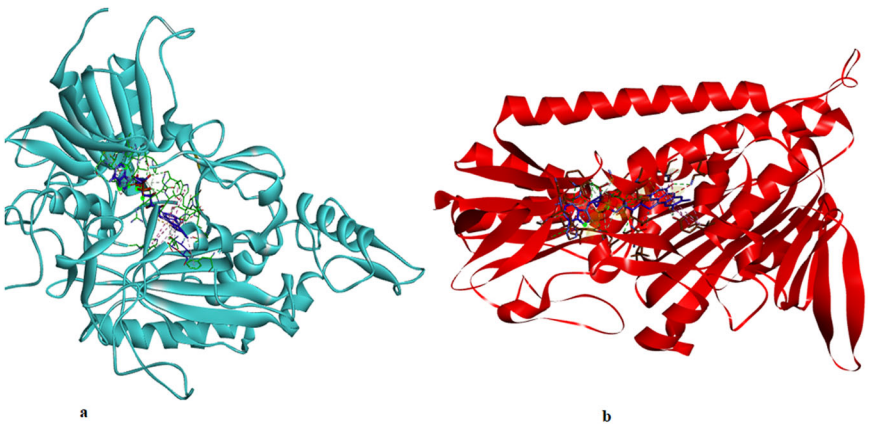

Fig. 2 Active site of AChE and GST. **a** AChE (PDB ID:4M0E), **b** GST (PDB ID:3DK9)

In silico pharmacokinetic profiling study

Osiris and Molinspiration analyses are performed to describe 2D models and to indicate the type of pharmacophore site [41]. These analyses are employed to predict the pharmacore site and biological activity of the 3-substitue 2-methyl indole analogs. Furthermore, the 3-substitue 2-methyl indole analogs determined some properties such as the drug-likeness score, steric effect, and electrostatic properties. In addition, these analyses report key features of the 3-substitue 2-methyl indole analogs-AChE/GST enzymes interactions. The Osiris/Molinspiration parameter values were identified via Cheminformatics free web services (http://www.molinspiration.com/cgi-bin/properties) and (https://www.organic-chemistry.org/prog/peo/). The pharmacokinetic and toxicity properties of the indole-triazole analogs were achieved by using the SwissADME which is an open online tool (http://www.swissadme.ch). The ADME properties define blood-brain barrier (BBB) permeability and passive human gastrointestinal absorption (HIA) as well as a substrate or non-substrate permeability glycoprotein (P-gp) and Cytochrome P450 (CYP) [42].

Compliance with ethical standards

Conflict of interest The authors declare no competing interests.

References

1. Mathew B, Parambi DG, Mathew GE, Uddin MS, Inasu ST, Kim H, et al. Emerging therapeutic potentials of dual-acting MAO and AChE inhibitors in Alzheimer's and Parkinson's diseases. Arch Pharm. 2019;352:1900177. https://doi.org/10.1002/ardp.201900177.
2. Li H, Su YS, He W, Zhang JB, Zhang Q, Jing XH, et al. The nonneuronal cholinergic system in the colon: a comprehensive review. FASEB J. 2022;36:e22165. https://doi.org/10.1096/fj.202101529R.
3. Taslimi P, Caglayan C, Gulcin İ. The impact of some natural phenolic compounds on carbonic anhydrase, acetylcholinesterase, butyrylcholinesterase, and α-glycosidase enzymes: An antidiabetic, anticholinergic, and antiepileptic study. J Biochem Mol Toxicol. 2017;31:e21995. https://doi.org/10.1002/jbt.21995.
4. Kalamida D, Poulas K, Avramopoulou V, Fostieri E, Lagoumintzis G, Lazaridis K, et al. Muscle and neuronal nicotinic acetylcholine receptors: structure, function and pathogenicity. FEBS J. 2007;274:3799–845. https://doi.org/10.1111/j.1742-4658.2007.05935.x.
5. Backos DS, Franklin CC, Reigan P. The role of glutathione in brain tumor drug resistance. Biochem Pharm. 2012;83:1005–12. https://doi.org/10.1016/j.bcp.2011.11.016.
6. Jefferies H, Coster J, Khalil A, Bot J, McCauley RD, Hall JC. Glutathione. ANZ J Surg. 2003;73:517–22. https://doi.org/10.1046/j.1445-1433.2003.02682.x.
7. Türkeş C, Demir Y, Beydemir Ş. Infection medications: assessment in-vitro glutathione S-Transferase inhibition and molecular docking study. ChemistrySelect. 2021;6:11915–24. https://doi.org/10.1002/slct.202103197.
8. Csermely P, Korcsmáros T, Kiss HJ, London G, Nussinov R. Structure and dynamics of molecular networks: a novel paradigm of drug discovery: a comprehensive review. Pharm Ther. 2013;138:333–408. https://doi.org/10.1016/j.pharmthera.2013.01.016.
9. Anderson AC. The process of structure-based drug design. Chem Biol. 2003;10:787–97. https://doi.org/10.1016/j.chembiol.2003.09.002.
10. Cetin A, Bursal E, Türkan F. 2-methylindole analogs as cholinesterases and glutathione S-transferase inhibitors: Synthesis, biological evaluation, molecular docking, and pharmacokinetic studies. Arab J Chem. 2021;14:103449. https://doi.org/10.1016/j.arabjc.2021.103449.
11. Suzen S. Recent studies and biological aspects of substantial indole derivatives with anti-cancer activity. Curr Org Chem. 2017;21:2068–76.
12. Singh TP, Singh OM. Recent progress in biological activities of indole and indole alkaloids. Mini Rev Med Chem. 2018;18:9–25.
13. Abele E, Abele R, Dzenitis O, Lukevics E. Indole and Isatin Oximes: synthesis, reactions, and biological activity. (Review). Chem Hetro Comp. 2003;39:3–35. https://doi.org/10.1023/A:1023008422464.
14. Suzen S, Cihaner SS, Coban T. Synthesis and comparison of antioxidant properties of Indole-based melatonin analogue Indole amino acid derivatives. Chem Biol Drug Des. 2012;79:76–83. https://doi.org/10.1111/j.1747-0285.2011.01216.x.
15. Mistry B, Keum YS, Kim DH. Synthesis, antioxidant and anticancer screenings of berberine-indole conjugates. Res Chem Intermed. 2016;42:3241–56. https://doi.org/10.1007/s11164-015-2208-x.
16. Bozorov K, Zhao J, Aisa HA. 1,2,3-Triazole-containing hybrids as leads in medicinal chemistry: a recent overview. Bioorg Med Chem. 2019;27:3511–31. https://doi.org/10.1016/j.bmc.2019.07.005.
17. Das A, Greco G, Kumar S, Catanzaro E, Morigi R, Locatelli A, et al. Synthesis, in vitro cytotoxicity, molecular docking and ADME study of some indolin-2-one linked 1, 2, 3-triazole derivatives. Comput Biol Chem. 2022;97:107641. https://doi.org/10.1016/j.compbiolchem.2022.107641.
18. Agalave SG, Maujan SR, Pore VS. Click chemistry: 1, 2, 3-triazoles as pharmacophores. Asian J Chem. 2011;6:2696–718. https://doi.org/10.1002/asia.201100432.
19. Narsimha S, Kumar NS, Swamy BK, Reddy NV, Hussain SA, Rao MS. Indole-2-carboxylic acid derived mono and bis 1,4-disubstituted 1,2,3-triazoles: Synthesis, characterization and evaluation of anticancer, antibacterial, and DNA-cleavage activities. Bioorg Med Chem Lett. 2016;26:1639–44. https://doi.org/10.1016/j.bmcl.2016.01.055.
20. Jasiewicz B, Kozanecka-Okupnik W, Przygodzki M, Warżajtis B, Rychlewska U, Pospieszny T, et al. Synthesis, antioxidant and cytoprotective activity evaluation of C-3 substituted indole derivatives. Sci Rep. 2021;11:1–14. https://doi.org/10.1038/s41598-021-94904-z.
21. Goyal D, Kaur A, Goyal B. Benzofuran and indole: promising scaffolds for drug development in Alzheimer's disease. Chem Med Chem. 2018;13:1275–99. https://doi.org/10.1002/cmdc.201800156.
22. Lan TT, Anh DT, Dung DTM, Huong LTT, Park EJ, Jeon HW, et al. Design, synthesis, and bioevaluation of novel oxoindolin-2-one derivatives incorporating 1-benzyl-1H-1,2,3-triazole. Med Chem Res. 2020;29:396–408. https://doi.org/10.1007/s00044-019-02488-1.
23. Sepehri N, Asemanipoor N, Mousavianfard SA, Hoseini S, Faramarzi MA, Adib M, et al. New acridine-9-carboxamide linked to 1,2,3-triazole-N-phenylacetamide derivatives as potent α-glucosidase inhibitors: design, synthesis, in vitro, and in silico biological evaluations. Med Chem Res. 2020;29:1836–45. https://doi.org/10.1007/s00044-020-02603-7.

24. Hein JE, Fokin VV. Copper-catalyzed azide–alkynecycloaddition (CuAAC) and beyond: new reactivity of copper(i) acetylides. Chem Soc Rev. 2010;39:1302–15. https://doi.org/10.1039/B904091A.
25. Meldal M, Tornøe CW. Cu-Catalyzed Azide-Alkyne Cycloaddition. Chem Rev. 2008;108:2952–3015. https://doi.org/10.1021/cr0783479.
26. Rostovtsev VV, Green LG, Fokin VV, Sharpless KB. A Stepwise Huisgen Cycloaddition Process: Copper(I)-Catalyzed Regioselective "Ligation" of Azides and Terminal Alkynes. Angew Chem Int Ed. 2002;114:2708–11.
27. Worrell BT, Malik JA, Fokin VV. Direct evidence of a dinuclear copper intermediate in Cu (I)-catalyzed azide-alkyne cycloadditions. Science. 2013;340:457–60. https://doi.org/10.1126/science.1229506.
28. Cetin A, Türkan F, Bursal E, Murahari M. Synthesis, characterization, enzyme inhibitory activity, and molecular docking analysis of a new series of Thiophene-based Heterocyclic compounds. Russ J Org Chem. 2021;57:598–604. https://doi.org/10.1134/S107042802104014X.
29. Aras A, Türkan F, Yildiko U, Atalar MN, Kılıç Ö, Alma MH, et al. Biochemical constituent, enzyme inhibitory activity, and molecular docking analysis of an endemic plant species, Thymus migricus. Chem Pap. 2021;75:1133–46. https://doi.org/10.1007/s11696-020-01375-z.
30. Güller P. The in vitro and in silico inhibition mechanism of glutathione reductase by resorcinol derivatives: a molecular docking study. J Mol Struct. 2021;1228:129790. https://doi.org/10.1016/j.molstruc.2020.129790.
31. Zhang MZ, Chen Q, Yang GF. A review on recent developments of indole-containing antiviral agents. Eur J Med Chem. 2015;89:421–41. https://doi.org/10.1016/j.ejmech.2014.10.065.
32. Kanwal KKM, Chigurupati S, Ali F, Younus M, Aldubayan M, Perveen S. Indole-3-acetamides: as potential antihyperglycemic and antioxidant agents; synthesis, in vitro α-amylase inhibitory activity, structure–activity relationship, and in silico studies. ACS Omega. 2021;6:2264–75. https://doi.org/10.1021/acsomega.0c05581.
33. Sravanthi TV, Manju SL. Indoles-A promising scaffold for drug development. Eur J Pharm Sci. 2016;91:1–10. https://doi.org/10.1016/j.ejps.2016.05.025.
34. Fraczek T, Siwek A, Paneth P. Assessing molecular docking tools for relative biological activity prediction: a case study of Triazole HIV-1 NNRTIs. J Chem Inf Model. 2013;53:3326–42. https://doi.org/10.1021/ci400427a.
35. Cetin A. In silico studies on stilbenolignan analogues as SARS-CoV-2 Mpro inhibitors. Chem Phys Lett. 2021;771:138563. https://doi.org/10.1016/j.cplett.2021.138563.
36. Schmidt AM, Eilbracht P. Tandem hydroformylation-hydrazone formation-Fischer indole synthesis: a novel approach to tryptamides. Org Biomol Chem. 2005;3:2333–43. https://doi.org/10.1039/B503396A.
37. Ellman GL, Courtney KD, Andres V Jr, Featherstone RM. A new and rapid colorimetric determination of acetylcholinesterase activity. Biochem Pharm. 1961;7:88–95.
38. Habig WH, Pabst MJ, Jakoby WB. J Biol Chem. 1974;249:7130–39. https://doi.org/10.1016/S0021-9258(19)42083-8.
39. Bhakta HK, Park CH, Yokozawa T, Min BS, Jung HA, Choi JS. Kinetics and molecular docking studies of loganin, morroniside and 7-O-galloyl-d-sedoheptulose derived from Corni fructus as cholinesterase and β-secretase 1 inhibitors. Arch Pharmacal Res. 2016;39:794–805. https://doi.org/10.1007/s12272-016-0745-5.
40. Morris GM, Huey R, Lindstrom W, Sanner MF, Belew RK, Goodsell DS, et al. AutoDock4 and AutoDockTools4: automated docking with selective receptor flexibility. J Comput Chem. 2009;30:2785–91. https://doi.org/10.1002/jcc.21256.
41. Hadda TB, Ali MA, Masand V, Gharby S, Fergoug T, Warad I. Tautomeric origin of dual effects of N1-nicotinoyl-3-(4′-hydroxy-3′-methyl phenyl)-5-[(sub)phenyl]-2-pyrazolines on bacterial and viral strains: POM analyses as new efficient bioinformatics' platform to predict and optimize bioactivity of drugs. Med Chem Res. 2013;22:1438–49. https://doi.org/10.1007/s00044-012-0143-6.
42. Moroy G, Martiny VY, Vayer P, Villoutreix BO, Miteva MA. Toward in silico structure-based ADMET prediction in drug discovery. Drug Disco Today. 2012;17:44–55. https://doi.org/10.1016/j.drudis.2011.10.023.

Publisher's note Springer Nature remains neutral with regard to jurisdictional claims in published maps and institutional affiliations.

Springer Nature or its licensor holds exclusive rights to this article under a publishing agreement with the author(s) or other rightsholder(s); author self-archiving of the accepted manuscript version of this article is solely governed by the terms of such publishing agreement and applicable law.